The development of a Planetary Broadband Seismometer (PBBS) for the Lunar Geophysical Network and the Ocean Worlds

Talso Chui

Jet Propulsion Laboratory, California Institute of Technology

12/14/2017

A NASA Funded Project thru the MaTISSE Program

PI:	Talso Chui (382), Technology
JPL Co-I:	Kedar Sharon (335), Science
	Inseob Hahn (382), Technology
U. Maryland Co-I:	Ho Jung Paik, Technology
	Nicholas Schmerr, Science
Austin Sensor Co-I:	Roger Williamson, Electronics
Staff Technologist:	Kistjan Stone
UCLA Student:	David Shelton
Collaborators:	Bruce Banerdt (JPL), Steve Vance (JPL),
	Clive Neal (U. Notre Dame).

Outline

- Background.
- Key Technology: Electrostatic Frequency Reduction (EFR)
- Mechanical Design.
- Electronics Design and Packaging
- Noise Budget

Background

- The International Lunar Network (ILN) Science Definition Team identified that future lunar seismometers should be ~10 X more sensitive than current SOA (2009).
- The Lunar Geophysical Network (LGN) identified as high value New Frontiers-class mission concept by NRC. Published Mission Concept Study (Shearer et al., 2011).
  - — 4 Landers, 1 orbiter.
- MatISSE proposal funded to develop an advanced seismometer for the next New Frontiers proposal cycle (~2021) and also for Ocean Worlds mission concepts.
- Possible earlier deployment on commercial lunar landers.

ILN Requirements Versus Current SOA

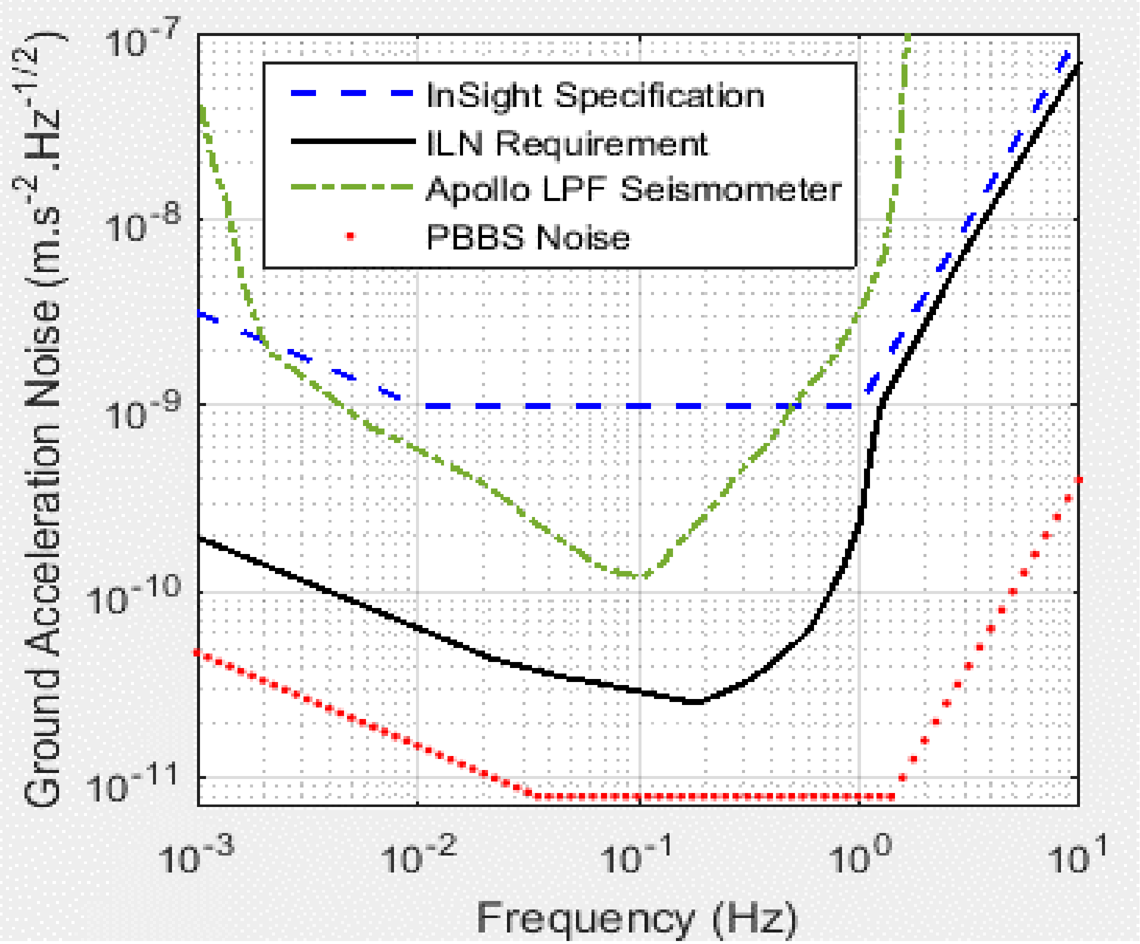

The Electrostatic Frequency Reduction Technology

- Force between two capacitor plates with area *A* and separated by a gap of *d* is:

$$\frac{\epsilon_o V^2 A}{2d^2}$$

ϵ_o is vacuum permeability

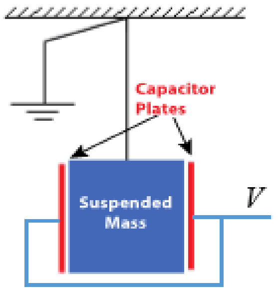

Figure 4: Frequency zeroing by counteracting the pendulum restoring force with electrostatic force.

- When displaced from the center by a displacement *x*, the force on the pendulum is.

$$F(x) = -\frac{\epsilon_o V^2 A}{2(d+x)^2} + \frac{\epsilon_o V^2 A}{2(d-x)^2} - k_{eff}x, \qquad k_{eff} = \frac{mg}{\ell}$$

- The Spring constant of the combined system is:

$$k_{total} = -\left.\frac{dF(x)}{dx}\right|_{x=0} = -\frac{2\epsilon_o V^2 A}{\mathrm{d}^3} + k_{eff}.$$

Resonance Frequency

$$f_o = \frac{1}{2\pi}\sqrt{\frac{k_{total}}{m}}$$

- Voltage required to bring the resonance frequency to zero is:

$$V = \sqrt{\frac{k_{eff} d^3}{2\epsilon_o A}}$$

~150 V for our case

Three Advantages for Reducing f_o

Seismometer is most sensitive when ground moves at a frequency >f_o, where the test mass is stationary and the electronics measured the displacement between the two

1. When the ground moves at frequencies < f_o, the test mass moves with the ground and there is little displacement between the two to be measured. Hence low f_o increases low frequency sensitivity.
2. High frequency seismic waves attenuates quickly with distance. Sensitivity at low frequency enables detection of weak sources from far away or from deep interior of the planetary body.
3. The Brownian motion noise of the test mass is lower with reduced f_o.

$$|a_\omega| = \sqrt{8\pi k_B T f_o/(mQ)}$$

- Additional Advantage of EFR: Remote or Autonomous Adjustment Possible

Mechanical Design

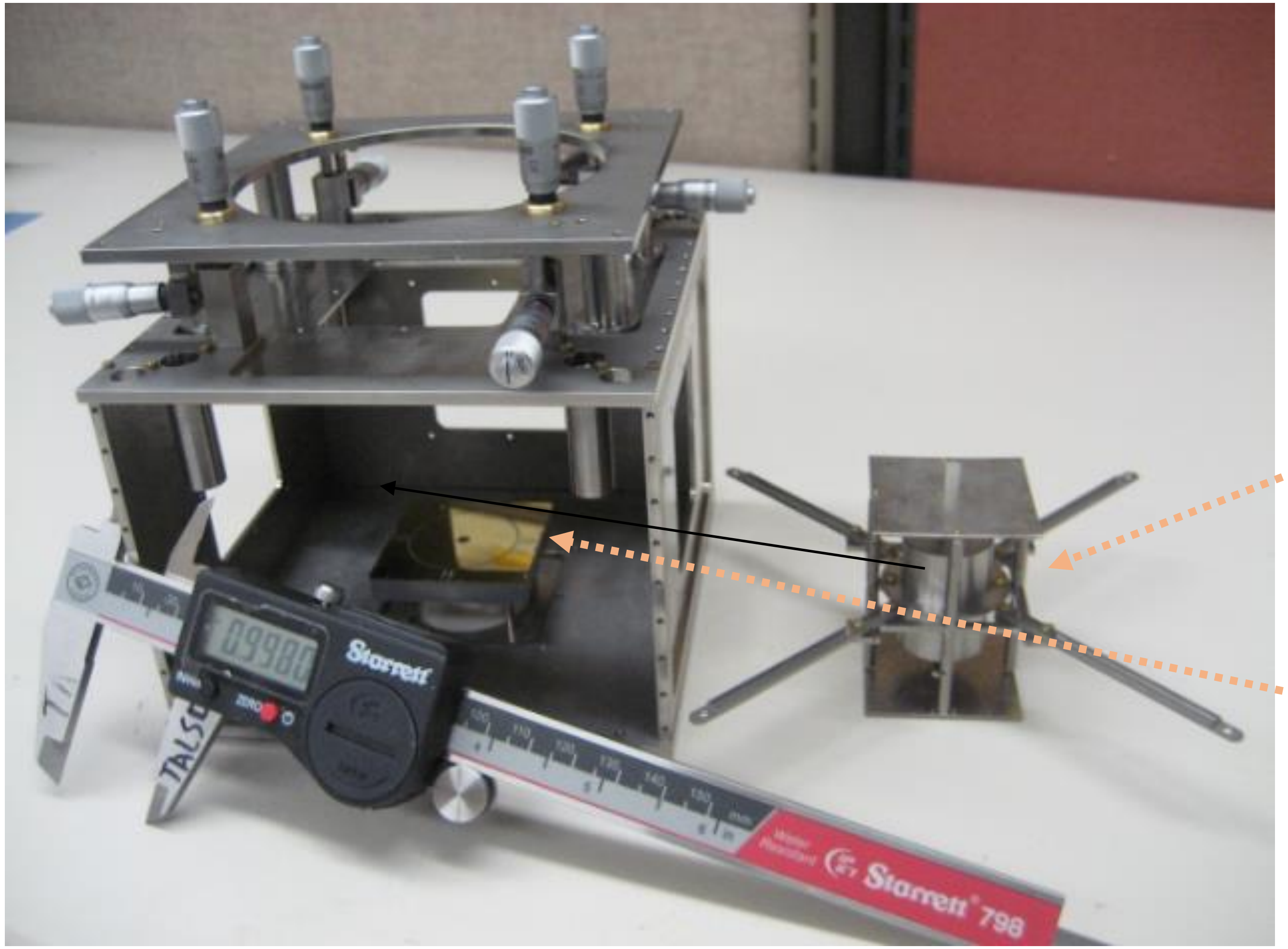

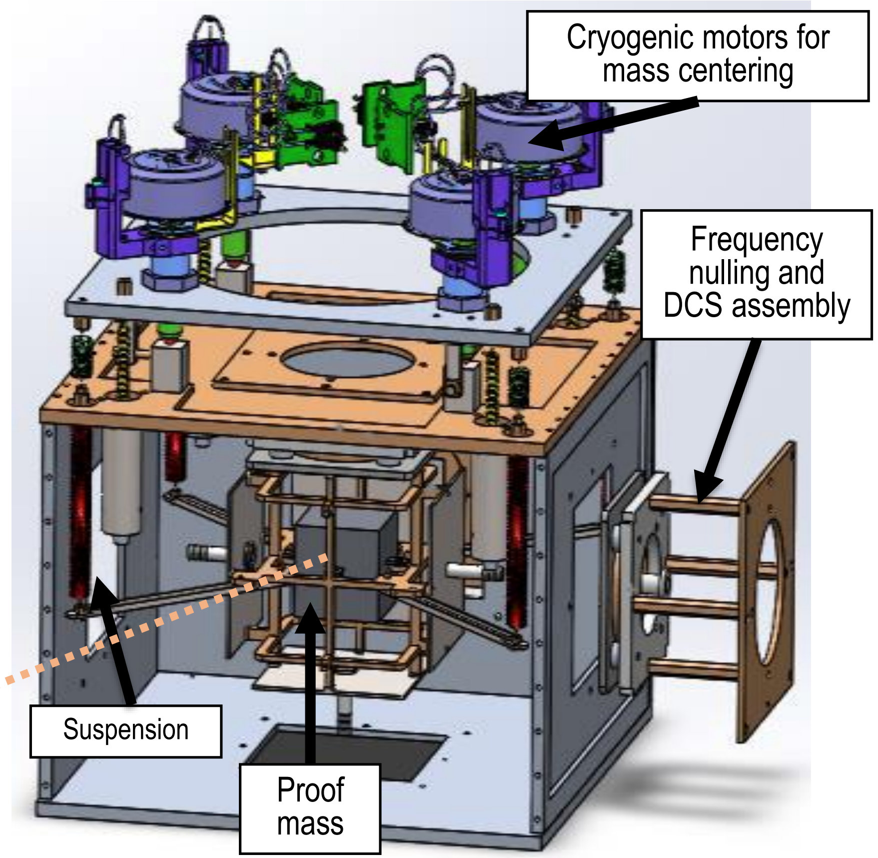

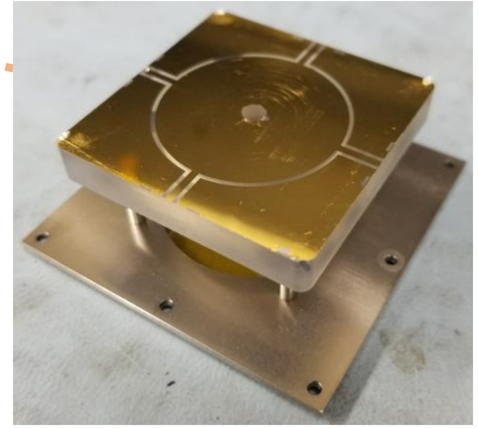

Zerodur Readout Capacitor Plate Design

Highlight of Mechanical Design

- High degrees of symmetry about the center of mass of test mass.
  - Coupling to rotational modes due to misalignments are reduced to second order effects.
- Use high density tungsten test mass to reduce moment of inertia m_R.
- Suspension points are separated as far away as practical.
  - This increases the restoring torque and hence the rotational spring constant k_R.
- Higher rotational modes frequencies means stiffness against rotation.
  - Rocking mode $f_o = 9$ Hz
  - Torsional mode $f_o = 4.5$ Hz

$$f_o = \frac{1}{2\pi}\sqrt{\frac{k_R}{m_R}}$$

- Use Ni-SPAN-C spring for low temperature coefficient.

Measurement of Temperature Coefficient of the Spring

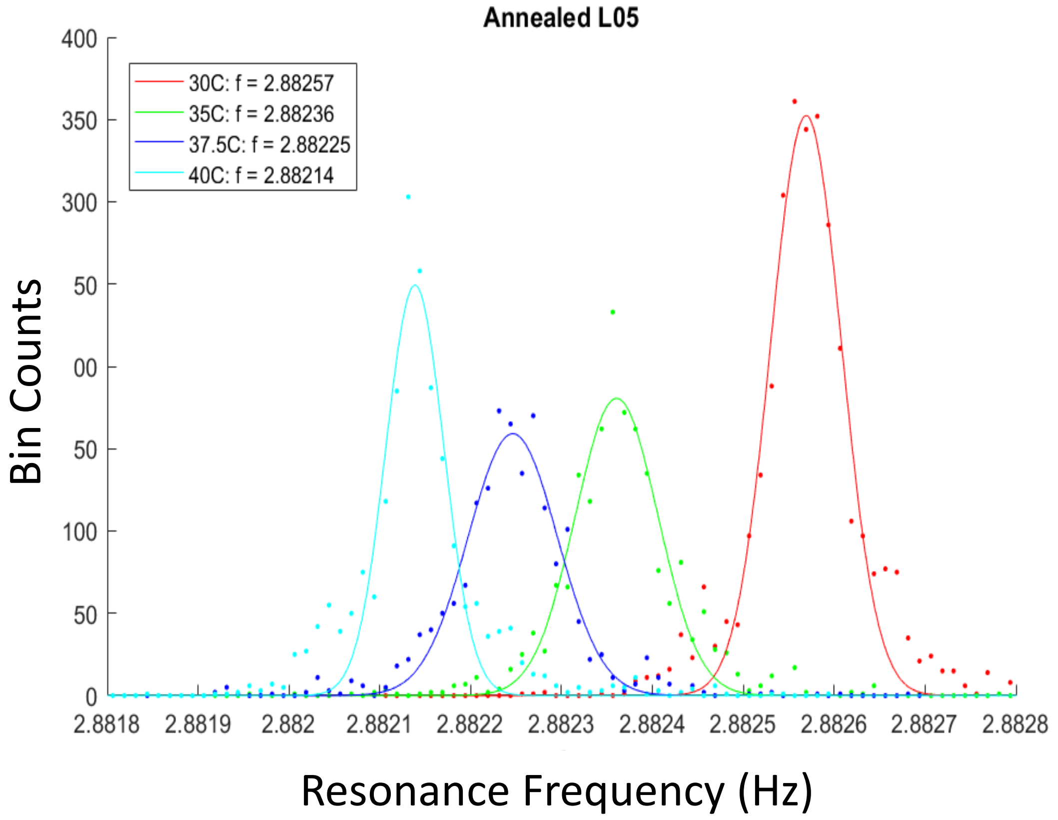

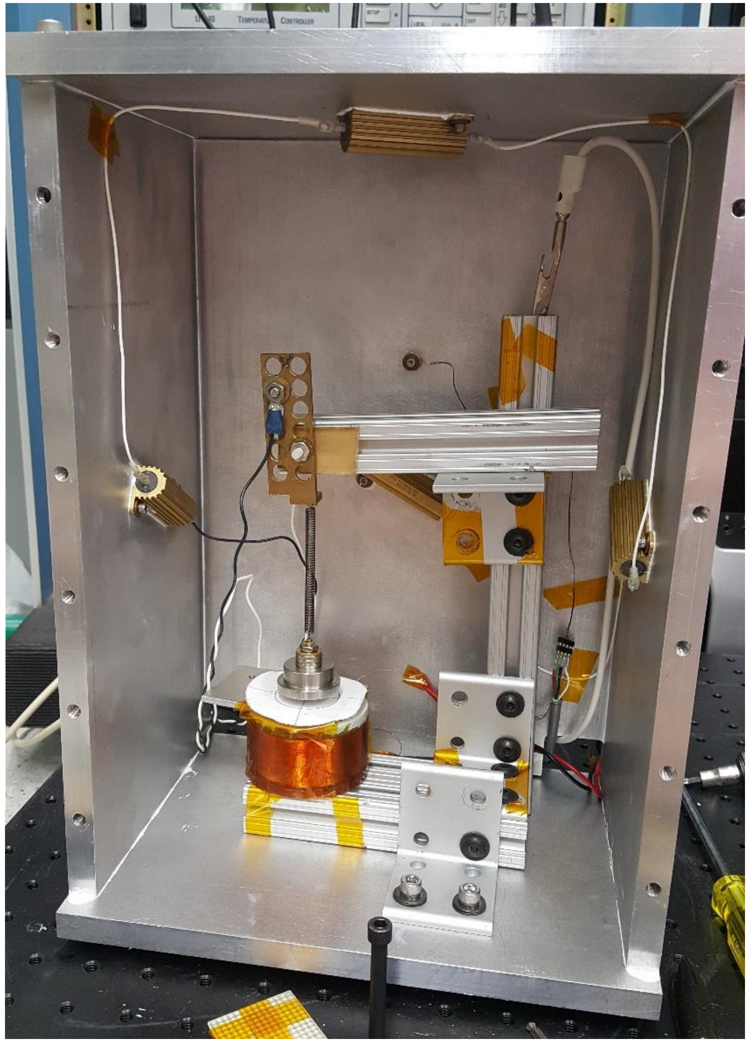

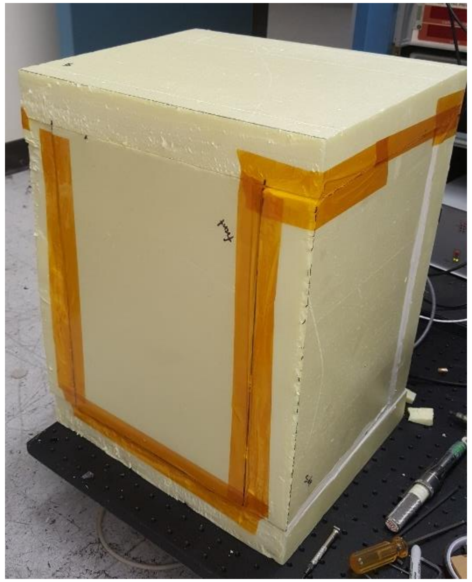

Spring Constant Temperature Coefficient = 30 ppm/^{o}C

Displacement Sensor Output is Proportional to Displacement

$$V_{DET} = NV_d\left(\frac{Z_2}{Z_1+Z_2}-\frac{1}{2}\right),$$

$$Z_1 = 1/(i\omega C_1),$$

$$Z_2 = 1/(i\omega C_2)$$

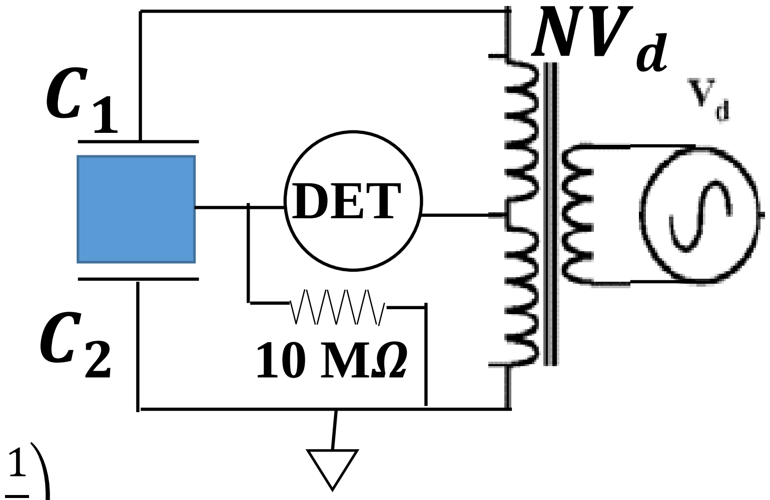

$$V_{DET} = NV_d\left(\frac{1/C_2}{1/C_1+1/C_2}-\frac{1}{2}\right),$$

$$C_1 = \epsilon_o\, A_{DCS}/(d_{DCS}-x) \qquad C_2 = \epsilon_o\, A_{DCS}/(d_{DCS}+x)$$

$$V_{DET} = NV_d\left(\frac{d_{DCS}-x}{2d_{DCS}}-\frac{1}{2}\right) = \frac{-NV_d x}{2d_{DCS}}$$

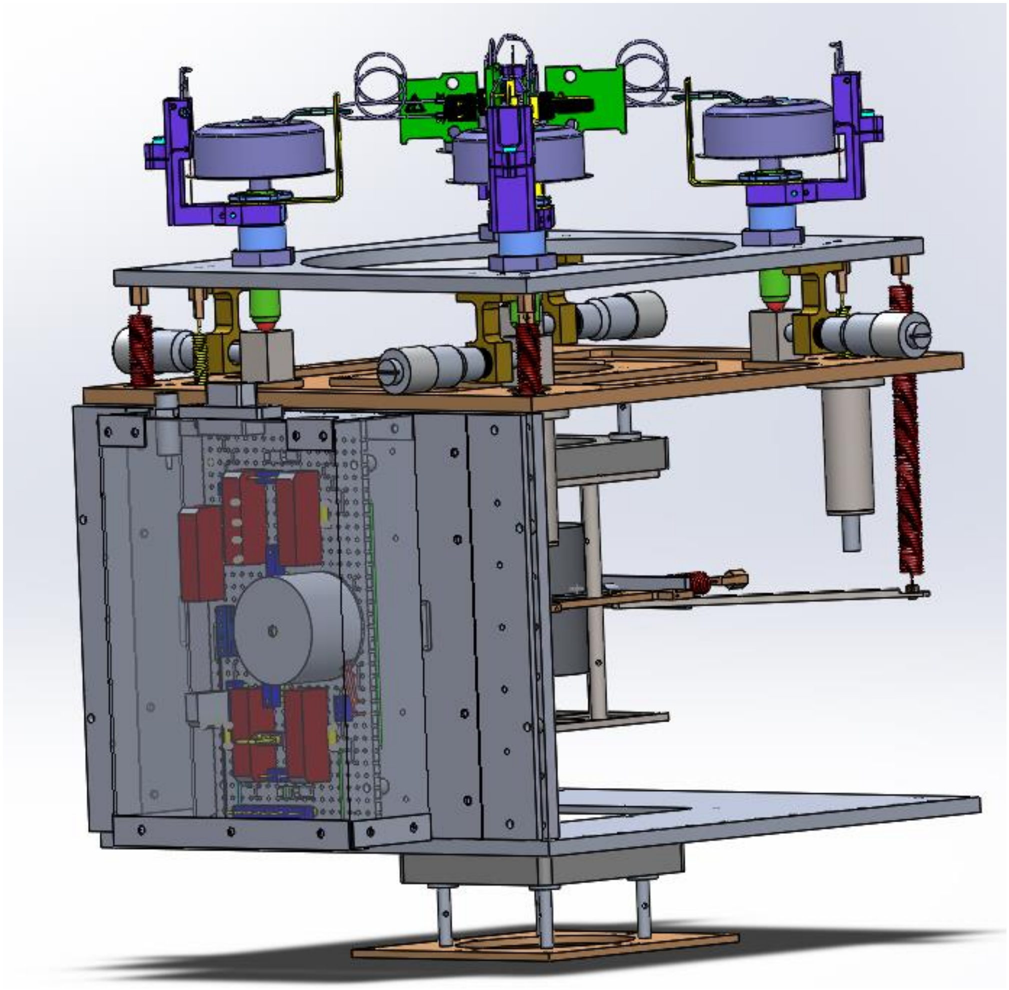

Packaged to be symmetric between top and bottom capacitor plates to minimize the effect of stray capacitance

DCS Noise with two 68 pf Capacitors to Simulate Test Mass Capacitances

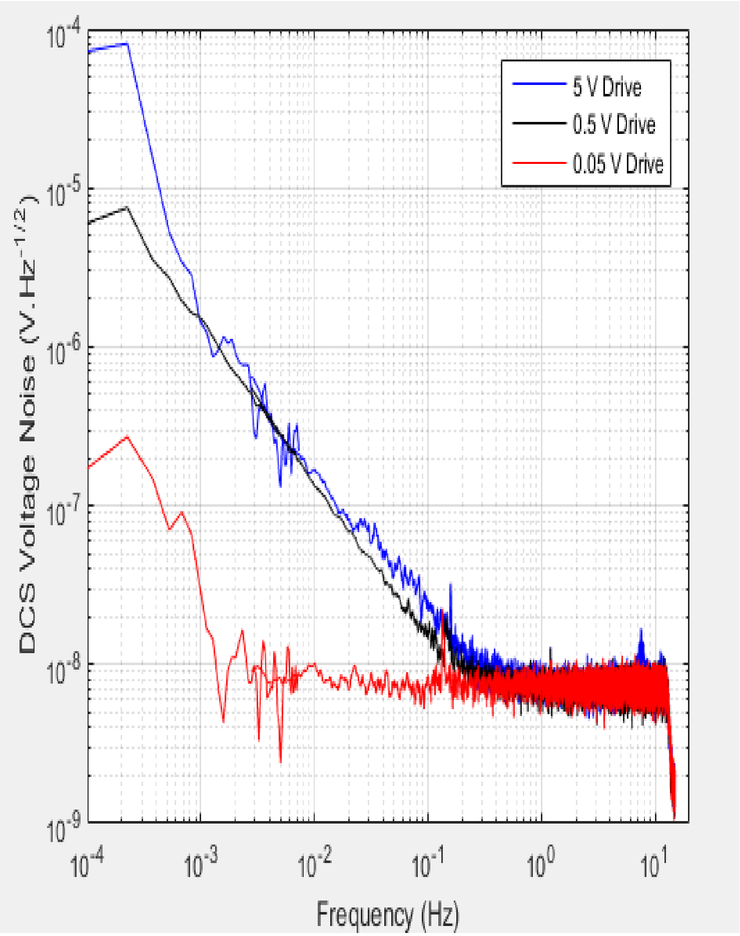

In Voltage Units

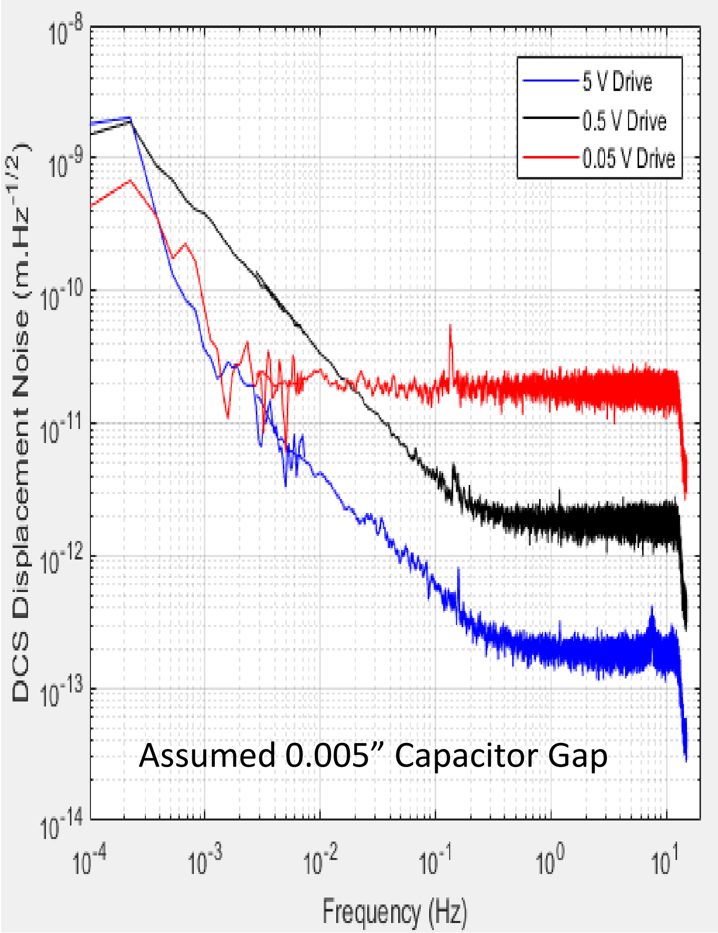

In Displacement Units

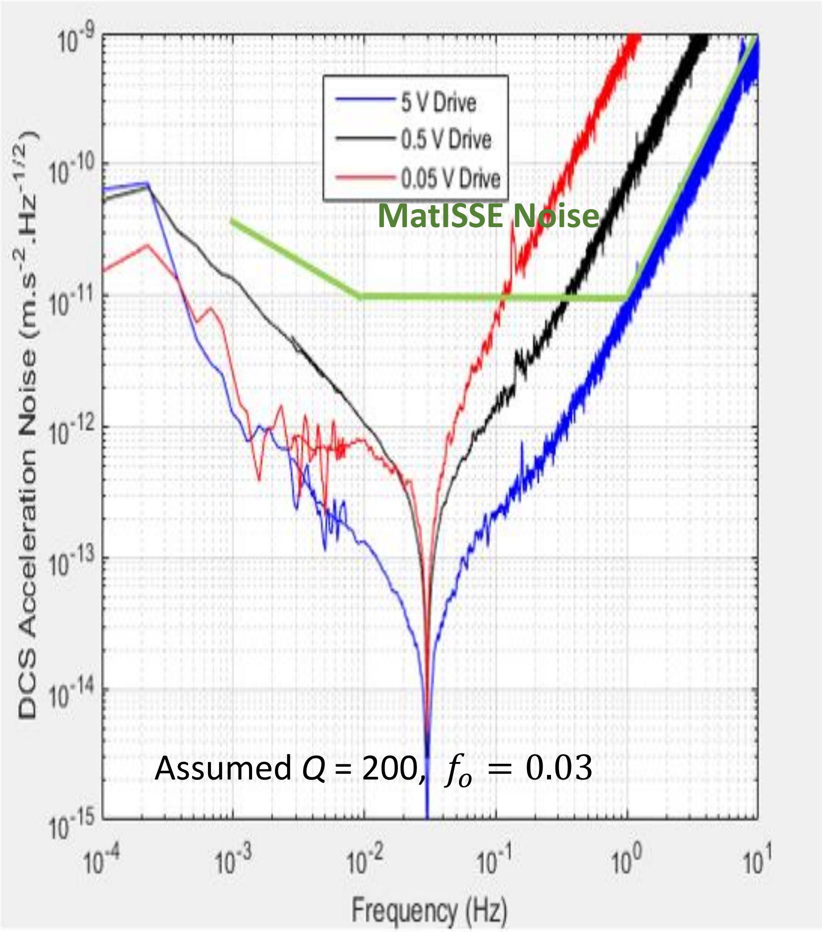

In Ground Acceleration Units

$$|a_\omega| = |x_\omega - X_\omega| \sqrt{(\omega_o^2 - \omega^2)^2 + (\omega\omega_o/Q)^2},$$

Seismometer Noise

Equation of Motion: $k(x - X) - H(\dot{x} - \dot{X}) + F(t) = m\ddot{x},$

Expressed in terms of spring mass oscillator parameters:
$k = m\omega_o^2, H = m\omega_o/Q, Q$ is quality factor.

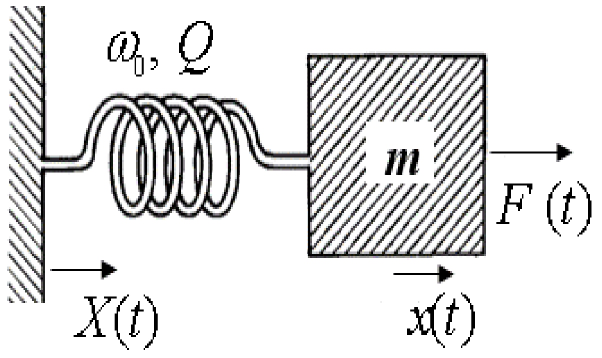

Time Domain: $\omega_o^2(x - X) \mp \frac{\omega_o}{Q}(\dot{x} - \dot{X}) + (\ddot{x} - \ddot{X}) = \frac{F(t)}{m} - \ddot{X}$

Frequency Domain: $\frac{F_\omega}{m} - a_\omega = \left(\omega_o^2 - \omega^2 \mp \frac{i\omega_o\omega}{Q}\right)(x_\omega - X_\omega)$

Voice Coil Noise & Brownian Noise

Displacement Sensor Noise

Brownian Noise: $|a_\omega| = \sqrt{8\pi k_B T f_o/(mQ)}$

Voice Coil Noise: $|a_{FB\_\omega}| = |V_{FB\_\omega}|E/(mR_s)$,

E is the current to force transfer coefficient of the voice coil.

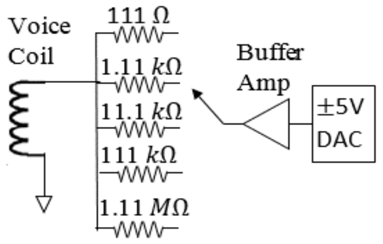

Voice Coil Drive

Displacement Sensor Noise:

$$|a_\omega| = |x_\omega - X_\omega|\sqrt{(\omega_o^2 - \omega^2)^2 + (\omega\omega_o/Q)^2},$$

$\omega \ll \omega_o$ $\quad |a_\omega| = \omega_o^2|x_\omega - X_\omega|$

$\omega \gg \omega_o$ $\quad |a_\omega| = \omega^2|x_\omega - X_\omega|$

EFR reduces low frequency DCS Noise.
At high frequencies, DCS Noise dominates.

Noise Budget:

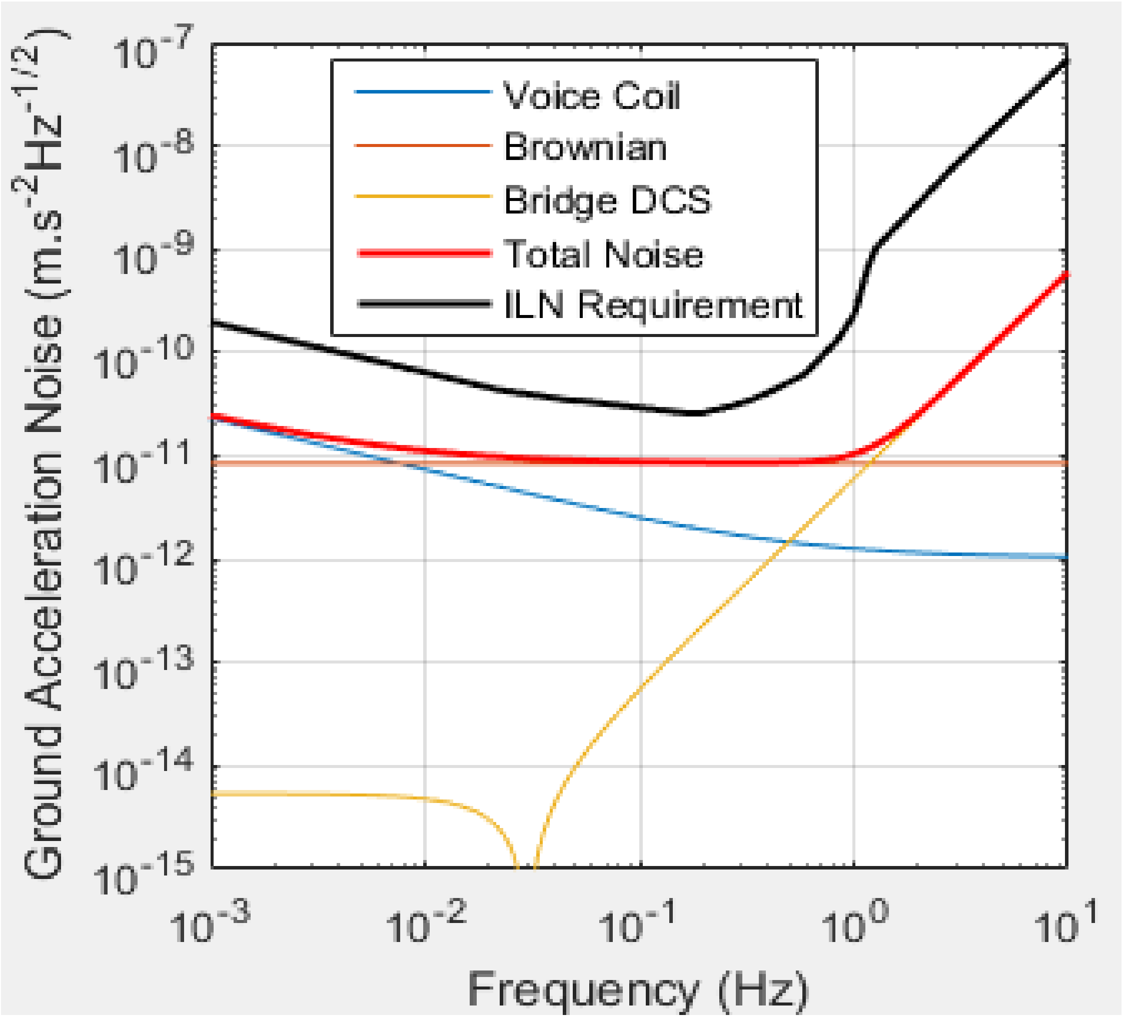

Backup Slides

Three Configurations for Flight Campaign

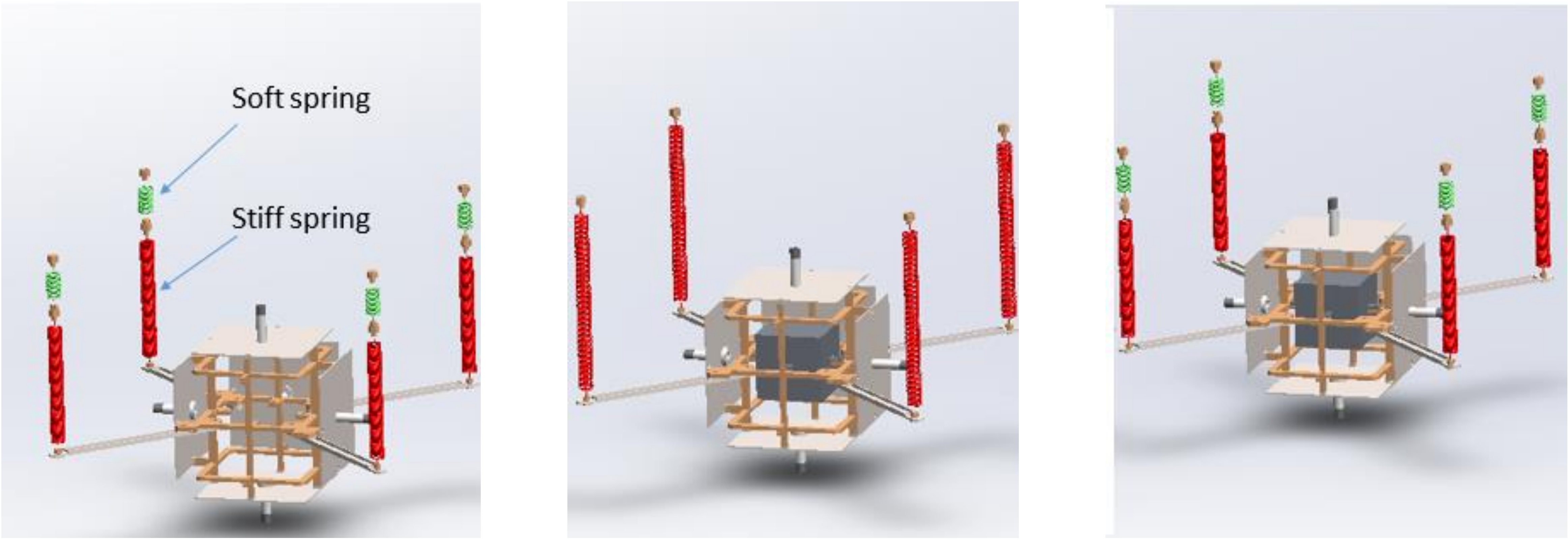

(a) (b) (c)

(a) Test mass frame has ~1/6 the mass of total suspended mass, add soft springs to simulate lunar gravity.

(b) Test with full test mass and stiff springs.

(c) Add soft springs prior to launch. May perform limited testing by off-loading.

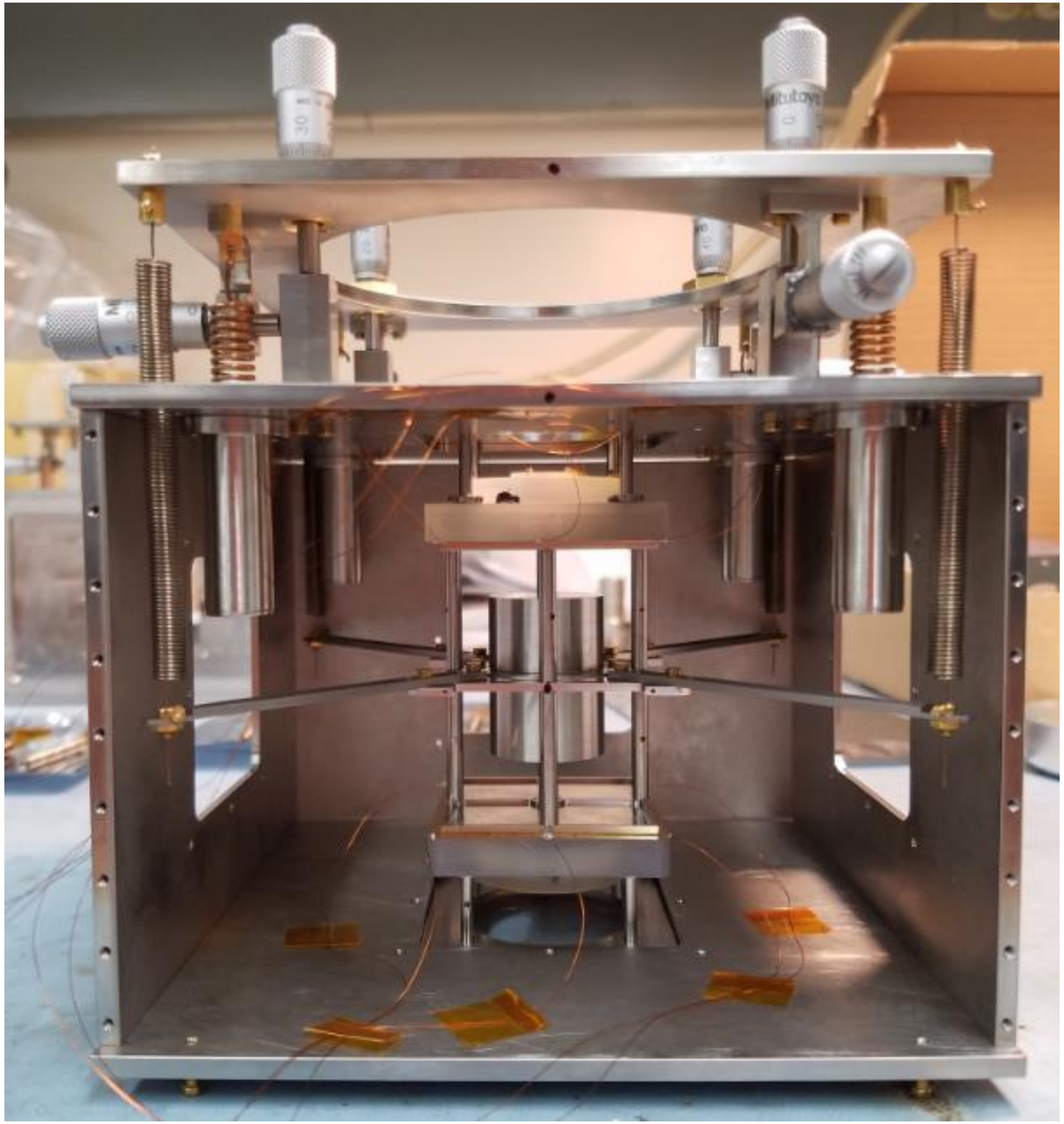

Cryogenic Pre-amplifier Ordered

Stahl-electronics.com, Model NexGen3 KC05 du V.09

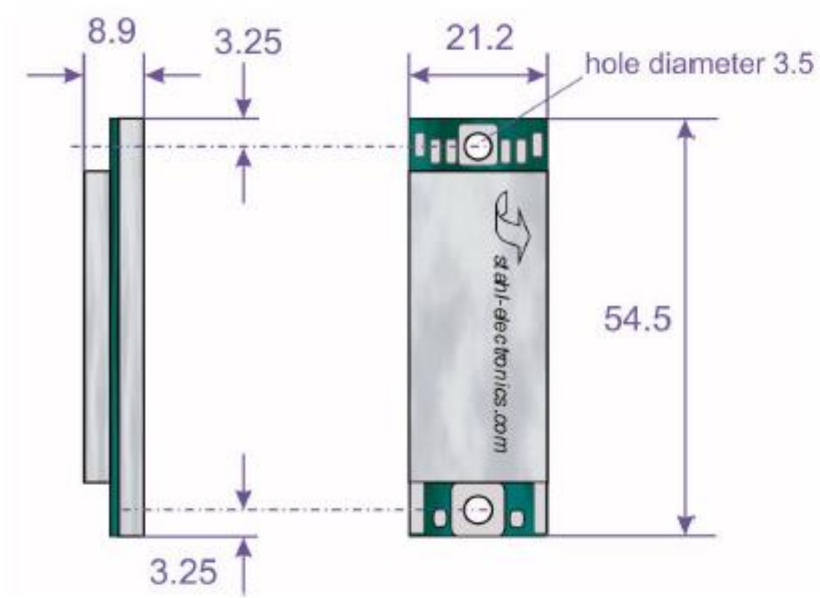

Figure 17: Outline dimensions (unit: mm)

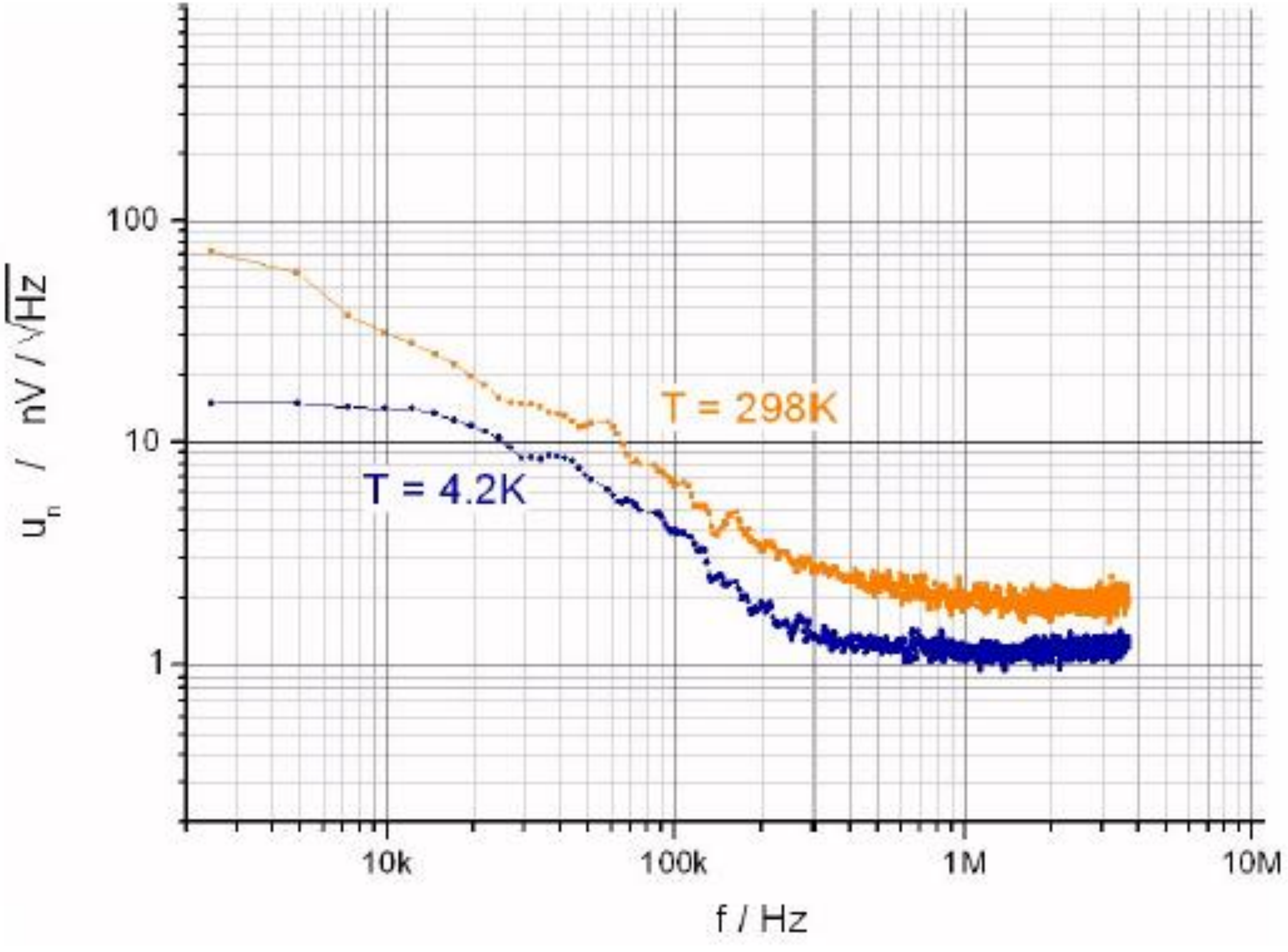

$12K

25 MΩ input impedance

10 fA/$\sqrt{Hz}$ current noise

Relative Permeability of Vitrovac Transformer Core

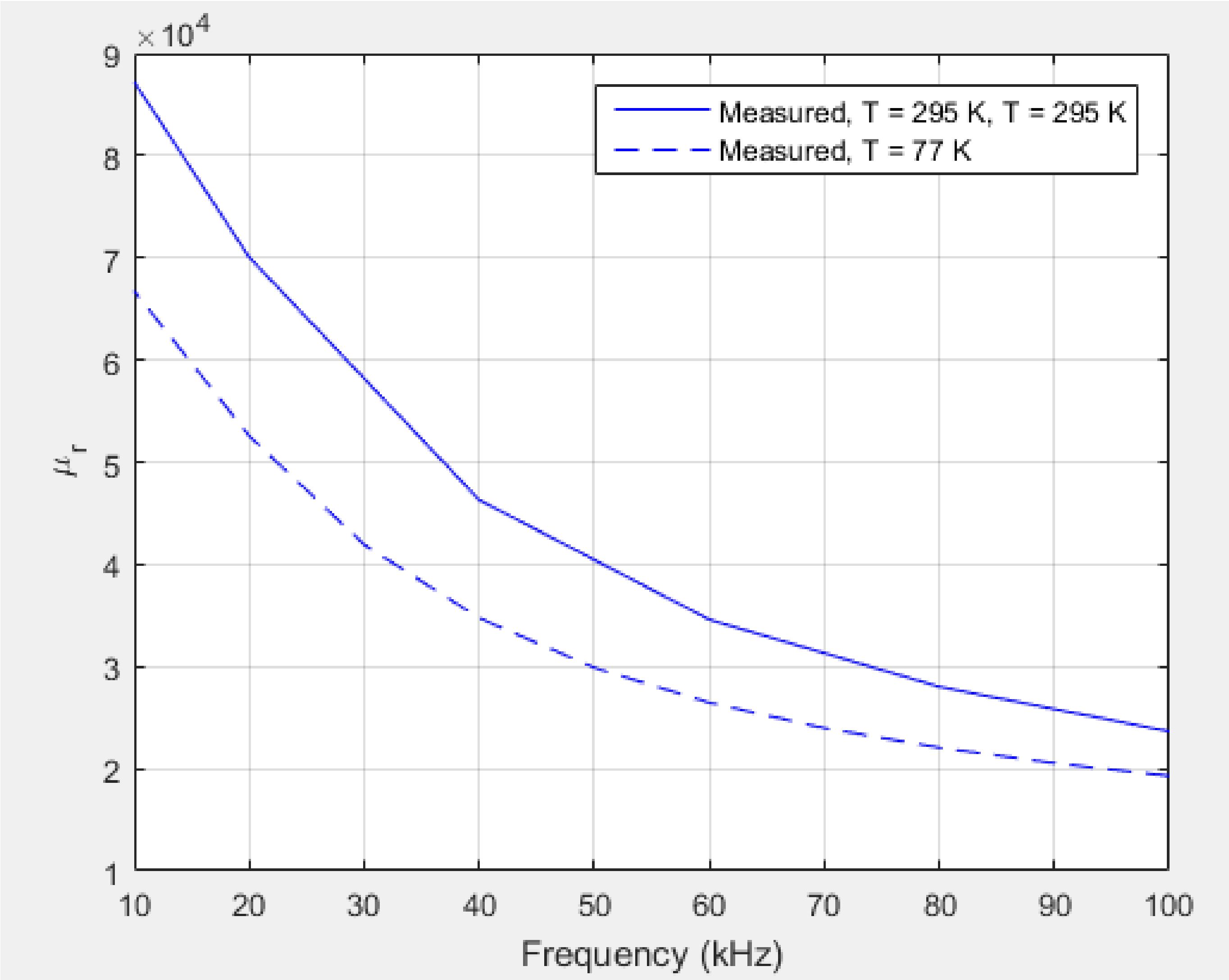

Cryogenic Test Facility Dewar Installed
Cryogenic Probe Ordered

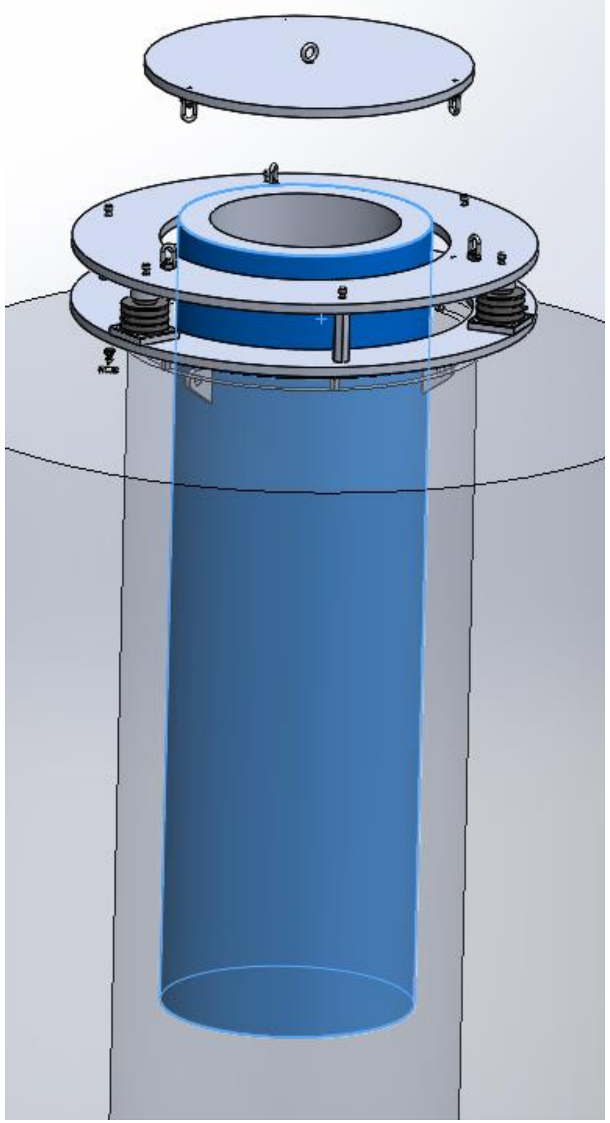

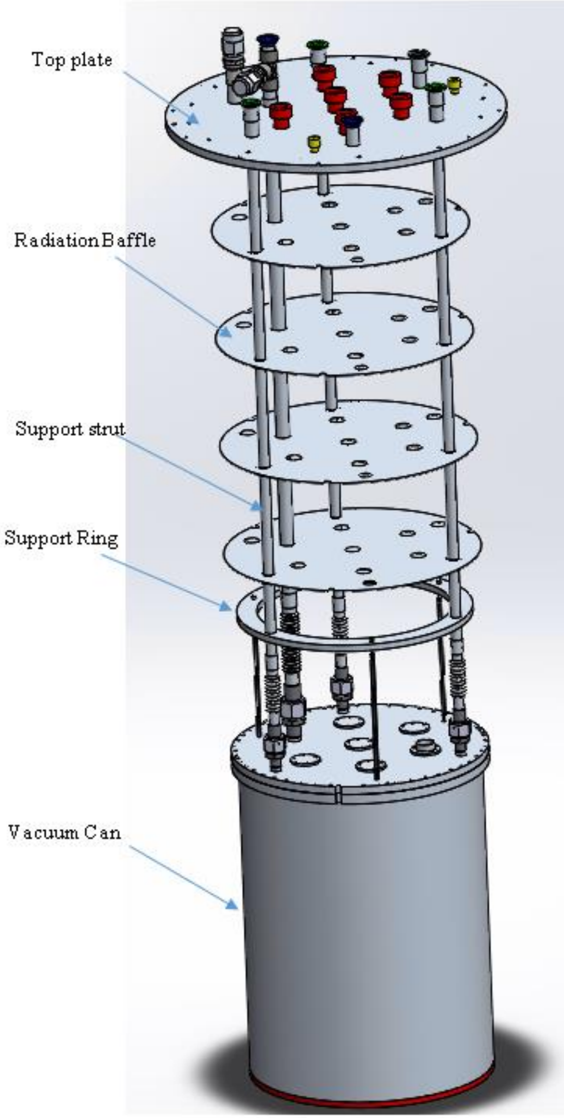

Capacitance Bridge Implementation

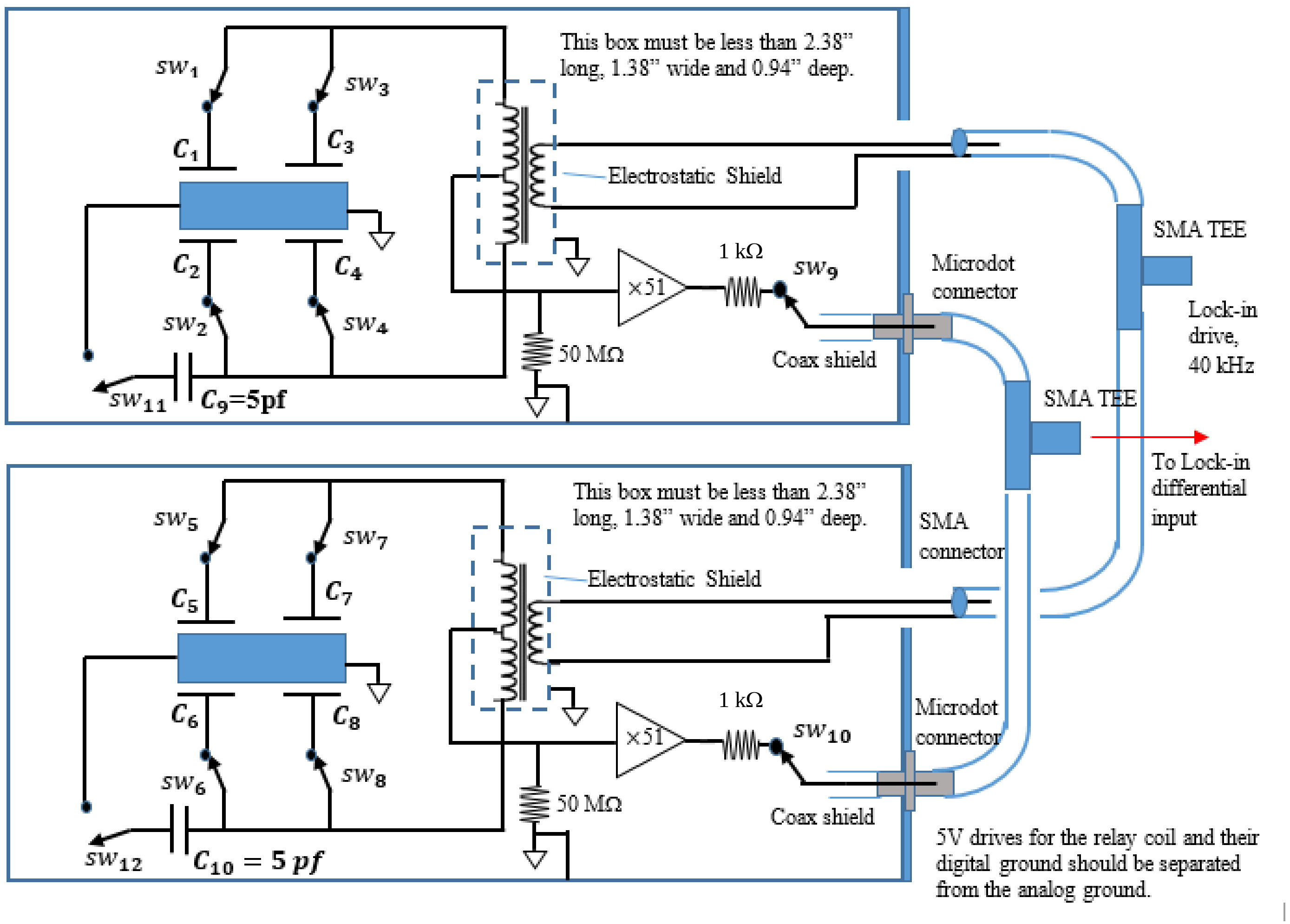

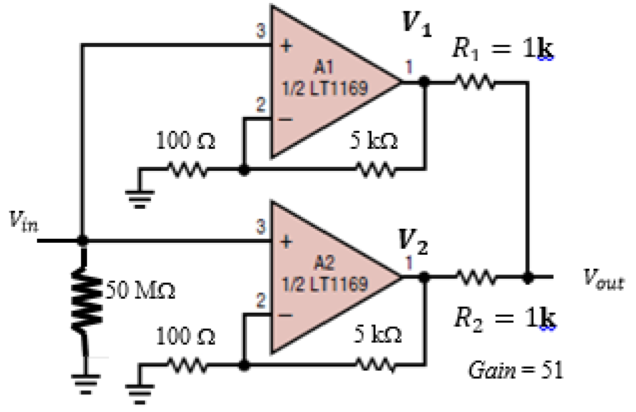

X 51 Amplifier with LT1169

LT1169

Voltage noise 6 nV/$\sqrt{Hz}$

Current noise 1 fA/$\sqrt{Hz}$

Displacement Sensor Output is Proportional to Displacement

$$V_{DET} = NV_d\left(\frac{Z_2}{Z_1+Z_2} - \frac{1}{2}\right),$$

$$Z_1 = 1/(i\omega C_1),$$

$$Z_2 = 1/(i\omega C_2)$$

$$V_{DET} = NV_d\left(\frac{1/C_2}{1/C_1+1/C_2} - \frac{1}{2}\right),$$

$$C_1 = \epsilon_o\, A_{DCS}/(d_{DCS} - x) \qquad C_2 = \epsilon_o\, A_{DCS}/(d_{DCS} + x)$$

$$V_{DET} = NV_d\left(\frac{d_{DCS}-x}{2d_{DCS}} - \frac{1}{2}\right) = \frac{-NV_d x}{2d_{DCS}}$$

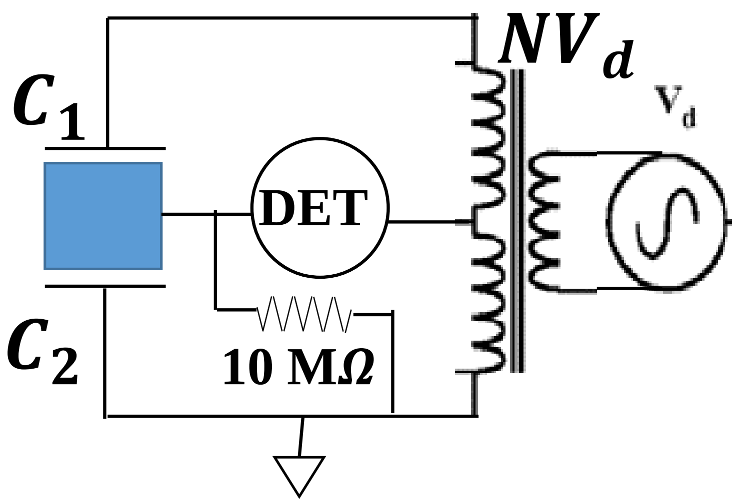

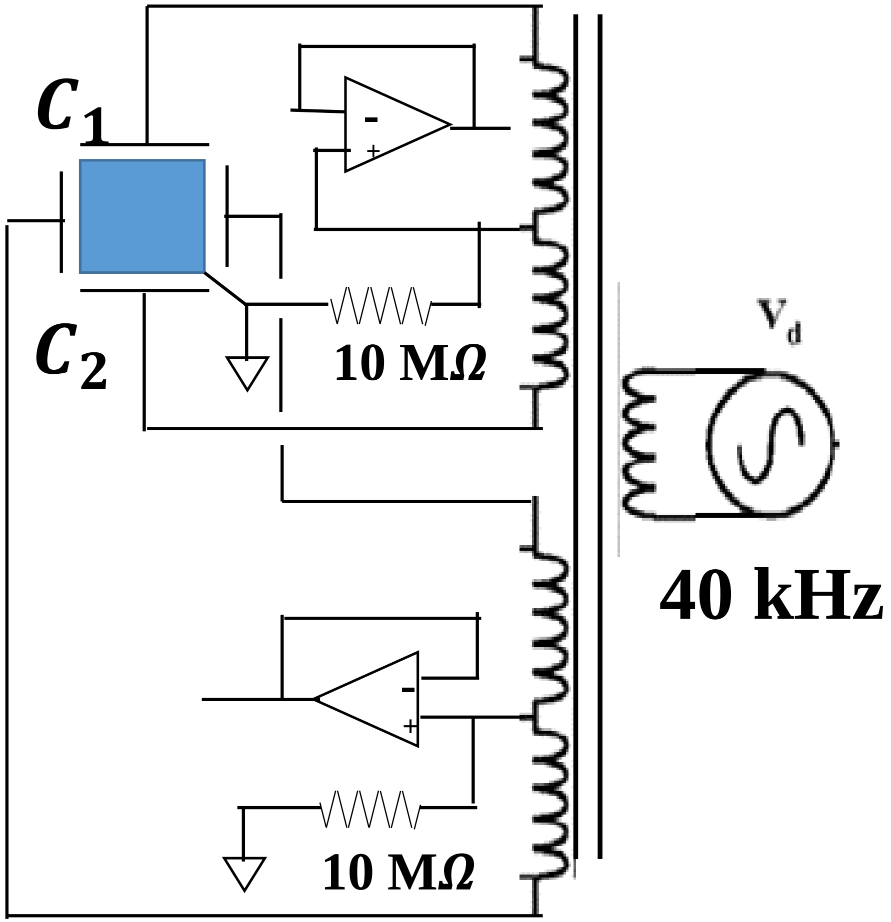

Changing ground does not change the performance

New Spring Suspension to allow increased degrees of freedom for adjustment.